

A HIGH FREQUENCY ULTRASOUND ELASTOGRAPHY SYSTEM FOR IN VIVO SKIN ELASTICITY IMAGING

M. Vogt⁺, S. Scharenberg[#], R. Scharenberg[#], K. Hoffmann^{*}, P. Altmeyer^{*}, and H. Ermert⁺

+Institute of High Frequency Engineering, Ruhr-University, Bochum, Germany

#taberna pro medicum GmbH, Lüneburg, Germany

*Dermatological University Hospital, Bochum, Germany

Michael.Vogt@rub.de

Abstract

The mechanical properties of the skin are of great relevance because they reflect the skin's constitution. In recent years, elastography has been successfully introduced as a tool for the spatially resolved measurement of tissue elasticity utilizing ultrasound at frequencies below 10 MHz. We have developed a 22 MHz ultrasound elastography system for high resolution skin elasticity imaging in vivo. In our setup, a vacuum is applied at the skin surface to cause an external deformation. Spatially resolved axial and lateral strains in the skin are derived analyzing high frequency echo signals, applying the 'phase root seeking' algorithm, and tracking speckles in B-mode images in axial and lateral direction. In this paper, the design of our system, the implemented strain estimation approaches and results from in vivo measurements are presented. Furthermore, a concept for the validation of the calculated strain estimates based on the correlation coefficient is proposed.

Introduction

Various skin diseases like psoriasis and scleroderma, as well as skin ageing and changes of the epidermal hydration cause changes of the skin elasticity. For this reason, tactually investigations are routinely performed in dermatology, but the results strongly depend on the individual sense of the physician. Different techniques for skin elasticity assessment have been introduced into dermatological

research. However, all these techniques suffer from the fact, that only skin *surface* deformations are assessed under an external deformation (traction, torsion, suction). High frequency ultrasound as well as optical coherence tomography (OCT) are tools which allow high resolution *imaging* of the skin [1,2]. Diridollou et al. assessed elastic skin properties applying high frequency ultrasound, analyzing skin layers contours deformations [3,4]. In 1991, ultrasound elastography was introduced by Ophir et al. as a modality to *image* local *strains* inside the tissue that are caused applying an external stress [5]. Cohn et al. applied high frequency ultrasound elastography for the analysis of tissue samples [6-8].

A high frequency ultrasound elastography system

We have implemented a high frequency ultrasound elastography system, working in the 20 MHz range, for high resolution in vivo imaging of skin elasticity [9]. The setup is based on a commercial ultrasound scanner (DUB 20, taberna pro medicum GmbH, Lüneburg, Germany) with a mechanically moved single element transducer, see Fig.1. The skin is sucked into the ultrasound applicator, applying a stepwise increased negative pressure at the skin surface. A digital pressure control loop was implemented for accurate and reproducible conditions. At each pressure, radio frequency (rf) echo signal frames are consecutively acquired over depth z and over the lateral coordinate x , see Fig. 2.

Strain estimation from tissue displacements

The suction at the skin surface causes displacements of the tissue structures over the depth z as well as the lateral coordinate x , see Fig. 2.



Figure 1: The implemented high frequency ultrasound elastography system: Applicator

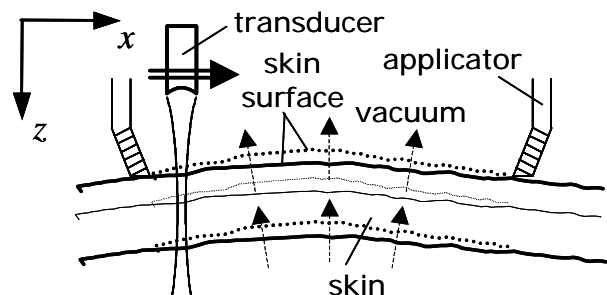


Figure 2: Vacuum applied at the skin surface sucks the skin into the ultrasound applicator: Depth z , lateral coordinate x

Relative displacements in local environments with respect to both coordinates are measures of the axial and lateral strains. To assess the relative displacements inside the tissue, the skin *surface* is used as a ‘seed point’ for tracking tissue displacements. Therefore, in a first step, the skin surface has to be segmented, which we perform with threshold segmentation, considering the ‘smoothness’ of the skin surface. Relative displacements *inside* the skin are iteratively assessed in windowed echo signal data over depth.

The segmented skin surface contours deliver already some information about the ‘overall’ skin elasticity. However, to *image* the elasticity over depth, strains *inside* the skin are determined analyzing backscattered ultrasound waves. Local axial and lateral strains are the derivatives of the estimated displacements over the axial and lateral coordinates. The distribution of the local strains represents the skin elasticity and, therewith, allows to distinguish between ‘hard’ (large strains) and ‘soft’ (small strains) tissue, presumed the mechanical *stress* inside the tissue is homogeneous. We have implemented two different displacement estimation approaches, that are based on the analysis of rf echo signals [9] and B-mode data.

Phase sensitive axial strain estimation

Axial displacements $\Delta z = c/2 \cdot \Delta t$ are equivalent to shifts Δt of the time of flight, that are scaled by the speed of sound c , see Fig. 3. We estimate these shifts by phase sensitive cross correlation of the analytical echo signals $s_{\text{echo}1+}(t)$ and $s_{\text{echo}2+}(t)$, that are acquired at the same lateral scan position x but with different negative pressures applied at the skin surface, i.e. at different external skin deformations:

$$c_{s1+,s2+}(t) = \int_{\tau} s_{\text{echo}1+}(\tau) \cdot s_{\text{echo}2+}^*(t + \tau) d\tau \quad (1)$$

Presumed the correlation between both signals is high, i.e. $s_{\text{echo}2+}(t) = s_{\text{echo}1+}(t - \Delta t)$, the *phase* of the *complex* cross correlation function $c_{s1+,s2+}(t)$ depends on the time of flight shift Δt :

$$c_{s1+,s2+}(t) = e^{-j\omega_0 \cdot (t - \Delta t)} \cdot \int_{\tau} s_0(\tau) \cdot s_0^*(t + \tau - \Delta t) d\tau \quad (2)$$

In this equation, $s_0(t)$ is the baseband signal of the analytical high frequency echo signal $s_{\text{echo}+}(t) = s_0(t) \cdot \exp(j\omega_0 \cdot t)$ with the carrier signal frequency ω_0 . The time shift Δt can be estimated very efficiently and accurately with an iterative search for the *root* of the phase of $c_{s1+,s2+}(t)$, which was

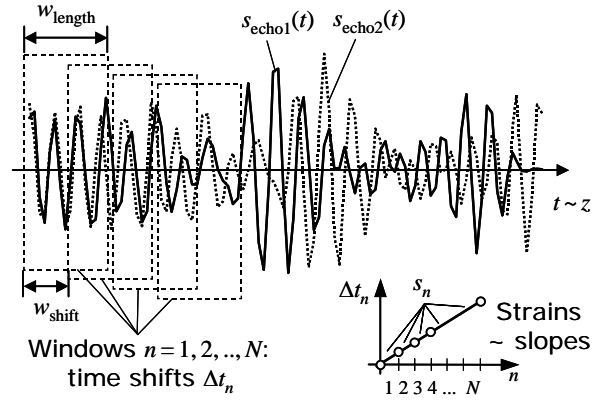


Figure 3: Phase sensitive axial strain estimation: Echo signals $s_{\text{echo}1}(t)$ and $s_{\text{echo}2}(t)$, window length w_{length} , window shift w_{shift} , time shifts Δt_n between echo signals in windows n , strain estimates s_n

proposed by Pesavento et al. (‘phase root seeking algorithm’) [10].

2D speckle tracking

In the second approach that we implemented, tissue displacements are tracked over depth z and over the lateral coordinate x . This is performed analyzing consecutive B-mode images $b(z, x)$, that are acquired during stepwise changed negative pressure applied at the skin surface. B-mode images are calculated as the magnitude of the analytical echo signals $s_{\text{echo}+}(t, x)$ at each lateral scan position x , with the time of flight t scaled by the speed of sound c , see Fig. 4:

$$b(z, x) = |s_{\text{echo}+}(z = c/2 \cdot t, x)| \quad (3)$$

Axial and lateral displacements Δz and Δx between two B-mode images $b_1(z, x)$ and $b_2(z, x)$ result in a linear *phase shift* between both corresponding spectra $B_1(\omega_z, \omega_x)$ and $B_2(\omega_z, \omega_x)$ as long as decorrelation between both B-mode images is negligible, i.e. $b_2(z, x) = b_1(z - \Delta z, x - \Delta x)$:

$$B_{1,2}(\omega_z, \omega_x) = \iint_{x, z} b_{1,2}(z, x) \cdot e^{-j(\omega_z \cdot z + \omega_x \cdot x)} dz dx \quad (4)$$

$$\Rightarrow B_2(\omega_z, \omega_x) = B_1(\omega_z, \omega_x) \cdot e^{-j\omega_z \cdot \Delta z} \cdot e^{-j\omega_x \cdot \Delta x}$$

Thus, displacements Δz and Δx can be estimated from the phase difference $\Delta\phi$ between both spectra:

$$\Delta\phi(\omega_z, \omega_x) = \arg \left\{ B_1(\omega_z, \omega_x) \cdot B_2^*(\omega_z, \omega_x) \right\} \quad (5)$$

$$\Rightarrow \Delta\phi(\omega_z, \omega_x) = \omega_z \cdot \Delta z + \omega_x \cdot \Delta x$$

Taking into account only the phase differences $\Delta\phi_v$ at spatial frequencies $\omega_{z,v}$ and $\omega_{x,v}$ with sufficiently high spectral energy, displacements estimates $\Delta\hat{z}_0$ and $\Delta\hat{x}_0$ estimates can be obtained by linear regression:

$$\sum_v (\Delta\phi_v - (\omega_{z,v} \cdot \Delta\hat{z}_0 + \omega_{x,v} \cdot \Delta\hat{x}_0))^2 = \min$$

$$\begin{pmatrix} \Delta\hat{z}_0 \\ \Delta\hat{x}_0 \end{pmatrix} = \begin{pmatrix} \sum_v \omega_{z,v}^2 & \sum_v \omega_{z,v} \cdot \omega_{x,v} \\ \sum_v \omega_{z,v} \cdot \omega_{x,v} & \sum_v \omega_{x,v}^2 \end{pmatrix}^{-1} \cdot \begin{pmatrix} \sum_v \omega_{z,v} \cdot \Delta\phi_v \\ \sum_v \omega_{x,v} \cdot \Delta\phi_v \end{pmatrix} \quad (6)$$

The limitation in this approach is, that the displacements must be small enough to obtain a non-ambiguous phase information, compare Fig. 4.

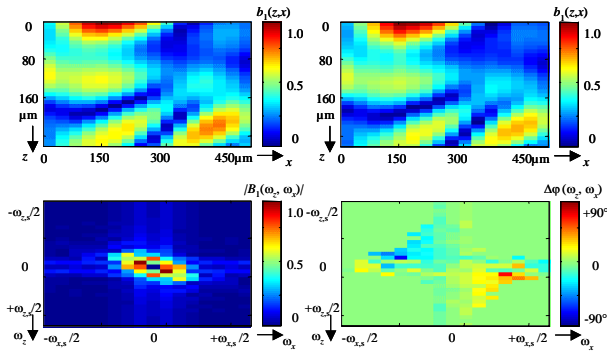


Figure 4: 2D speckle tracking: B-mode images $b_1(z,x)$ and $b_2(z,x)$, magnitude spectrum $|B_1(\omega_z, \omega_x)|$, phase difference $\Delta\phi(\omega_z, \omega_x)$ between spectra $B_1(\omega_z, \omega_x)$ and $B_2(\omega_z, \omega_x)$

Reliability of displacements and strain estimates

The above discussed displacement estimation approaches were introduced under the assumption, that only axial time shifts Δt (rf echo signals) and displacements Δz and Δx (B-mode images) occur as a result of the external tissue deformation. However, if local strains in the tissue are too high, the echo signals as well as the B-mode images might be decorrelated. But *reliable* displacement estimates are essential for the ability to determine axial and lateral strains. Therefore, we propose to calculate the correlation coefficients of the high frequency echo signals and of the B-mode images after the estimated displacements have been considered, and to use them as measures for the *reliability* of the estimated strains [9].

In vivo measurements

The implemented system was tested by measurements on speckle phantoms with varying elastic properties. Furthermore, the proposed strain estimation approaches were validated under defined conditions using simulated echo signals. In this paper, we present results from our clinical study, which was performed at healthy skin and skin lesions in vivo [9]. In the B-mode image in Fig. 5, which was acquired at the forearm, a nevus can be identified as an echo poor structure inside the echo rich dermis. Underneath, the subcutaneous fat is visible as a layered structure. A set of rf echo signal frames was acquired during a stepwise increased negative pressure inside the rectangular applicator aperture with a size of 12 mm x 6 mm. Pressure was changed by 12 mbar

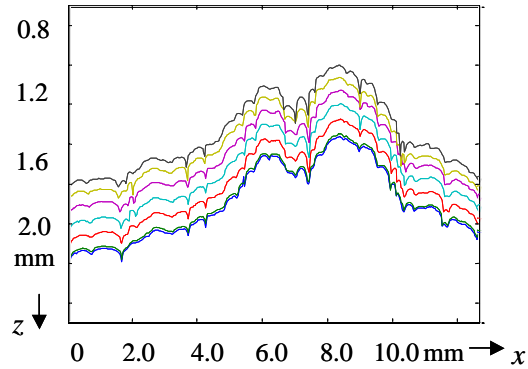
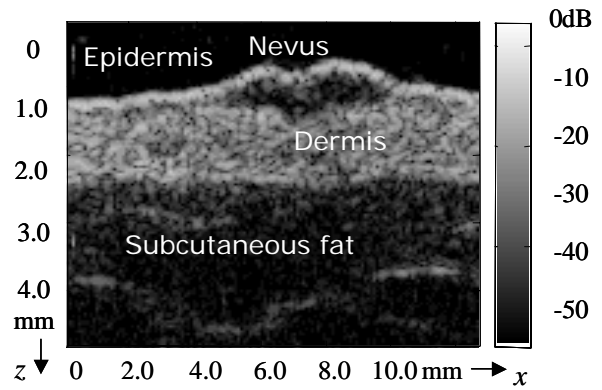


Figure 5: B-mode image (top), segmented skin surface contours during stepwise increased vacuum (bottom): Nevus at forearm

steps between consecutive scans. The skin surface was segmented in each frame, and the segmented contours are shown in Fig. 5. The graphs show that the axial displacement of the skin *surface* is very homogeneous over the lateral coordinate x .

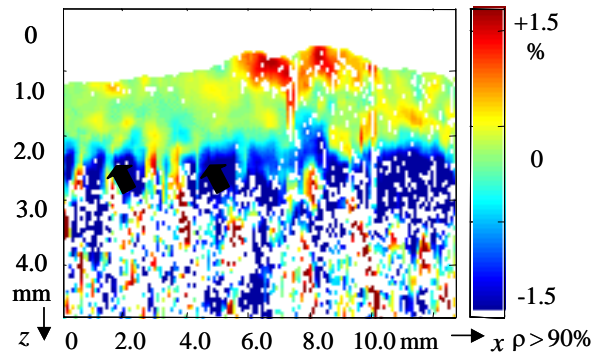


Figure 6: Phase sensitive axial strain estimate, gated estimates with correlation coefficients $\rho > 90\%$: Nevus at forearm

In Fig. 6 the phase sensitive axial strain estimate is shown, whereby only estimates with correlation coefficients $\rho > 90\%$ are visualized. Axial strains inside the dermis are small, whereas the subcutaneous fat is significantly *elongated* (negative strains). On the other hand, the nevus is significantly *compressed* (positive strains) and very small axial strains are found in the dermis. It can be concluded that the subcutaneous fat and the nevus are much softer than the dermis [9].

The 2D speckle tracking approach, which is proposed in this paper was applied to estimate the local axial and lateral strains based on the B-mode images, that were calculated from the rf echo signals.

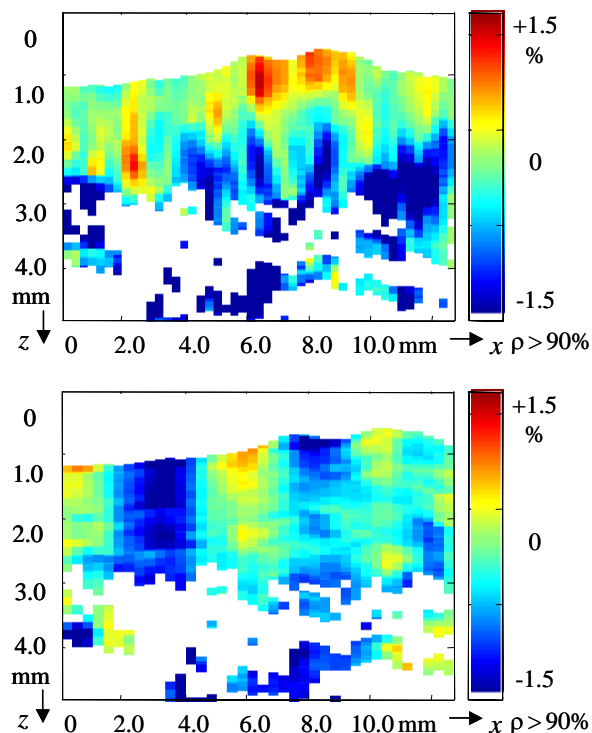


Figure 7: 2D speckle tracking strain estimates, gated estimates with correlation coefficients $\rho > 90\%$: Axial strain (top), lateral strain (bottom): Nevus at forearm

In Fig. 7 the estimated axial and lateral strains are shown. Again, only estimates with correlation coefficients $\rho > 90\%$ are visualized to obtain images with reliable data. The axial strain estimates are in a good agreement with the phase sensitive estimates in Fig. 6. The estimated lateral strains show a large elongation (negative strains) in some axially layered regions along the lateral coordinate x as well as regions of vanishing lateral strain. A plausible correlation between axial and lateral strain estimates is found in Fig. 7, as axial strains are found in regions with lateral strains and vice versa as well as corresponding regions with vanishing axial and lateral strains.

Summary and conclusions

In this paper the design and implementation of a high frequency ultrasound elastography system for in vivo skin elasticity assessment was presented. A phase sensitive approach based on rf signal analysis for axial strain estimation and a 2D speckle tracking approach based on B-mode data were implemented and applied to in vivo measurements results. It was shown that axial strain estimates from both approaches are in good agreement. Furthermore, speckle tracking allows to estimate lateral strains, whereby the reliability of all estimates was validated using the correlation

coefficient as a measure of reliability. Maximum axial strains of about 1.5% were obtained in our in vivo measurements with a stepwise 12mbar pressure change at the skin surface. The findings of our preliminary study show that high frequency ultrasound can be successfully applied to high resolution skin elasticity imaging in vivo.

Acknowledgements

A project of the Ruhr Center of Competence for Medical Engineering (KMR). Supported by the Federal Ministry of Education and Research, No. 13N8079.

References

- [1] M. Vogt, K. Kaspar, P. Altmeyer, K. Hoffmann, and S. El Gammal, "High frequency ultrasound for high resolution skin imaging," *Frequenz*, vol. 55, no 1-2, pp. 12-20, 2001.
- [2] M. Vogt, A. Knüttel, K. Hoffmann, P. Altmeyer, and H. Ermert, "Comparison of high frequency ultrasound and optical coherence tomography as modalities for high resolution and non invasive skin imaging," *Biomed. Technik*, vol. 48, no 5, pp. 116-121, 2003.
- [3] S. Diridollou, M. Berson, V. Vabre, D. Black, B. Karlsson, F. Auriol, J.M. Gregoire, C. Yvon, L. Vaillant, Y. Gall, and F. Patat, "An in vivo method for measuring the mechanical properties of the skin using ultrasound," *Ultras. in Med. & Biol.*, vol. 24, no 25, pp. 215-224, 1998.
- [4] S. Diridollou, F. Patat, F. Gens, L. Vaillant, D. Black, J.M. Lagarde, Y. Gall, and M. Berson, "In vivo model of the mechanical properties of the human skin under suction," *Skin Research and Technol.*, vol. 6, pp. 214-221, 2000.
- [5] J. Ophir, I. Céspedes, H. Ponnekanti, Y. Yazdi, and X. Li, "Elastography, a quantitative method for imaging the elasticity of biological tissues," *Ultrason. Imaging*, vol. 13, no 2, pp. 111-134, 1991.
- [6] N.A. Cohn, S.Y. Emelianov, M.A. Lubinski, and M. O'Donnell, "An elasticity microscope. Part I: Methods," *IEEE Trans. Ultrason. Ferroel. Freq. Contr.*, Vol. 44, No 6, pp. 1304-1319, 1997.
- [7] N.A. Cohn, S.Y. Emelianov, and M. O'Donnell, "An elasticity microscope. Part II: Experimental results," *IEEE Trans. Ultrason. Ferroel. Freq. Contr.*, vol. 44, no 6, pp. 1320-1331, 1997.
- [8] N.A. Cohn, B.S. Kim, R.Q. Erkamp, D.J. Mooney, S.Y. Emelianov, A.R. Skovoroda, and M. O'Donnell, "High-resolution elasticity imaging for tissue engineering," *IEEE Trans. Ultrason. Ferroel. Freq. Contr.*, vol. 47, no 4, pp. 956-966, 2000.
- [9] M. Vogt, S. Scharenberg, R. Scharenberg, K. Hoffmann, P. Altmeyer, and H. Ermert, "In vivo evaluation and imaging of skin elasticity applying high frequency (22 MHz) ultrasound," *2002 IEEE Ultrasonics Symposium Proceedings*, pp. 1819-1822, 2002.
- [10] A. Pesavento, C. Perrey, M. Krueger, and H. Ermert, "A time-efficient and accurate strain estimation concept for ultrasonic elastography using iterative phase zero estimation," *IEEE Trans. Ultrason. Ferroel. Freq. Contr.*, vol. 46, no 5, pp. 1057-1067, 1999.